The International Journal of Advanced Manufacturing Technology (2025) 137:5511–5520
https://doi.org/10.1007/s00170-025-15487-x

ORIGINAL ARTICLE

Effects of laser patterning and heat treatment on hydrophobicity, wear, and corrosion resistance of 316L stainless steel

Hsuan-Kai Lin[1] · Shang-Jen Yang[1] · Po-Wei Chang[1] · Wei-Hua Lu[1] · Yuan-Jen Chang[2]

Received: 31 December 2024 / Accepted: 27 March 2025 / Published online: 7 April 2025

Abstract

Many methods have been proposed to enhance the surface wettability of stainless steel to improve its wear and corrosion-resistant properties. However, these methods are often expensive and time-consuming. Accordingly, this study presents a straightforward approach for improving the surface wettability of 316L stainless steel using UV laser patterning at a wavelength of 355 nm, followed by heat treatment. The effects of the laser power (0.3–1.0 W), scanning speed (100–900 mm/s), heat treatment temperature (100–200 °C), and heat treatment duration (0–12 h) on the surface roughness, wettability, wear resistance, and corrosion resistance are systematically explored. The experimental results show that laser treatment at a scanning speed of 500 mm/s followed by heat treatment at 150 °C for 6 h produced a hydrophobic surface with a contact angle of 138.0°. The wear resistance of the sample was significantly improved, with a reduction in the friction coefficient from 0.075 to 0.059. The electrochemical tests showed that the hydrophobic surface reduced the corrosion current from 7.89E − 8 to 5.11E − 8 A/cm^2. Overall, the optimal laser modification (1 W- 500 mm/s) and post-heat treatment (150 °C) provide an effective approach for enhancing the hydrophobicity, wear resistance, and corrosion resistance of 316L stainless steel, thereby offering an efficient alternative to existing surface modification methods.

Keywords Laser modification · Stainless steel · Wettability · Wear resistance

1 Introduction

316L stainless steel is used in many industrial applications and plays a crucial role in aerospace, medical devices, and chemical equipment [1, 2]. However, 316L stainless steel surfaces are susceptible to wear and corrosion, which limit their long-term stability, performance, and broader applications. Consequently, improving the wear and corrosion resistance of 316L stainless steel through surface modification has emerged as a key challenge. Traditional methods for enhancing the surface properties, such as chemical treatment and coatings, often face limitations related to durability, cost, and environmental impact. In contrast, hydrophobic surfaces offer significant advantages, including superior corrosion resistance and self-cleaning properties [3]. Among the advanced techniques available for creating such surfaces, laser patterning technology has found extensive applications owing to its efficiency, versatility, and precision [4–11].

Wettability refers to the interaction between a liquid droplet and a material surface. For a liquid droplet in equilibrium on a surface, the wettability can be characterized by the magnitude of the contact angle of the droplet on the surface. Three models can be used to explain the wettability. Young's model [12] describes the ideal surface wettability and is given as.

$$\gamma_{LV}{}^{\cos\theta_e} = \gamma_{SV-}\gamma_{SL} \tag{1}$$

where γ_{LV}, γ_{SV}, and γ_{SL} are the liquid–gas, solid–gas, and solid–liquid surface tensions, respectively, and θ_e is the equilibrium contact angle.

However, Young's model is applicable only to perfectly flat and homogeneous surfaces. Thus, for non-smooth surfaces, it is replaced by the Wenzel model [13], which accounts for the surface roughness by assuming that the liquid fills the surface pores. The Wenzel model is formulated as follows:

✉ Hsuan-Kai Lin
HKLin@mail.npust.edu.tw

[1] Department of Materials Engineering, National Pingtung University of Science and Technology, Pingtung 912, Taiwan

[2] Department of Mechanical Engineering, National Taipei University of Technology, Taipei, Taiwan

$$\cos\ \theta_w = r\cos\ \theta_e \tag{2}$$

where θ_w is the contact angle of the droplet on the rough surface, and r is the surface roughness factor (defined as the ratio of the actual contact area of the droplet on the surface to the projected contact area). Surfaces with a contact angle of $\theta_e > 90°$ are defined as hydrophobic, whereas those with $\theta_e < 90°$ are defined as hydrophilic.

The Cassie-Baxter model [14] introduces the concept of a gas layer between the liquid and the surface and treats the surface as a solid–gas mixture. Thus, it is particularly suitable for superhydrophobic surfaces (i.e., surfaces with contact angles greater than 150°), such as solar panels, self-cleaning windows, anti-icing coatings, and medical devices [15]. Mathematically, the Cassie-Baxter model is written as.

$$\cos\ \theta_C = f_1 \cos\theta - f_2 \tag{3}$$

where θ_C is the contact angle of the droplet on the surface and f_1 and f_2 are the fractions of the surface in contact with solid and gas, respectively. If there are no gas pockets ($f_2 = 0$), the Cassie-Baxter model reduces to the Wenzel model.

Surface modification technologies such as laser patterning and electrodeposition, which produce high-energy metal oxides, cause the wettability of the surface to gradually change from hydrophilic to superhydrophobic over time [3, 16]. For example, Lin et al. [17] reported that pure Ti samples processed by high-pressure torsion, followed by annealing and laser surface treatment, underwent a hydrophilic-to-hydrophobic transformation during aging under ambient conditions, and reached a contact angle as high as 129° after 13 days. In a recent study [18], the same group showed that Ti and Ti64 samples processed using HPT followed by laser surface treatment initially exhibited a hydrophilic surface with a contact angle of approximately 10–13°, but transitioned to a hydrophobic surface with a contact angle of 120–126° after a holding time of 27 days. Several studies have reported that laser-textured surfaces initially exhibit hydrophilicity [17–20]. However, after a period of static placement or treatments such as silanization, oxygen plasma, or low-temperature annealing, the number of active functional groups reduces, thereby lowering the surface energy and enhancing the hydrophobicity [21]. Zhou et al. [22] investigated the use of femtosecond laser texturing to create micro-nano hybrid structures on titanium alloy, focusing on their effects on mechanical properties, wettability, and anti-reflective performance. It emphasized the critical role of the depth-to-width aspect ratio (D/W) in optimizing surface characteristics. The findings showed that femtosecond laser texturing minimally affects the alloy's ultimate tensile strength (UTS), with reductions ranging from only 0.16 to 3.27%, demonstrating excellent material stability. Moreover, an increase in the D/W ratio was associated with higher coefficients of friction and frictional forces, highlighting the influence of surface morphology on tribological performance. Enhanced D/W ratios also improve wettability and anti-reflective properties by increasing surface area, resulting in greater hydrophobicity and more effective internal reflections. Zhai et al. [23] explored the enhancement of hydrophobicity and tribological properties of 304 stainless steel through laser surface texturing (LST). Surface roughness measurements revealed that the CSA sample had a roughness of 13.893 μm, the CM5 sample exhibited 9.138 μm, and the CM2 sample showed the finest roughness at 3.212 μm. Wettability tests indicated that the CM2 sample displayed superior hydrophobicity, with a significantly higher contact angle than the CSA sample, demonstrating better water repellency. Tribological tests conducted under oil lubrication conditions revealed that the laser-treated samples had considerably lower friction coefficients compared to the untreated sample. Among them, the CM2 sample achieved the best tribological performance, with the lowest friction coefficient observed. These findings suggest that laser surface texturing is a highly effective technique for enhancing both hydrophobicity and tribological properties of 304 stainless steel, with the CM2 treatment offering the most optimized surface morphology for superior performance.

Several studies have shown that heat treatment accelerates the hydrophilic-to-hydrophobic transition. For example, Ngo et al. [24] reported that low-temperature annealing of a laser-patterned surface at 100 °C reduced the transition time from hydrophilic to hydrophobic from a couple of months to just several hours. Li et al. [8] showed that laser texturing of brass surfaces followed by heat treatment prompted the formation of a superhydrophobic surface as a result of the micro-/nanostructures produced by the laser texturing and adsorption of organic matter from the ambient air during heat treatment. Wang [25] similarly combined laser texturing and heat treatment to create Ti6Al4V samples with superhydrophobic surfaces. The results showed that the treatment process increased the contact angle from 64.8° (hydrophilic) to 155° (superhydrophobic). Notably, the superhydrophobic surface showed a greatly improved anti-corrosion performance compared to the original hydrophilic surface.

Residual stress is influenced by the heat input during processing [26]. Increasing the volumetric energy input, such as laser power or scan speed, generally results in higher residual stresses in materials. However, laser surface texturing (LST) requires lower power compared to other laser manufacturing processes, such as powder bed fusion or laser selective melting. As a result, it seldom requires post-treatment to eliminate residual stresses, nor is it typically discussed in related articles. Santos et al. [27] found that in the case of Ti-6Al-4 V alloy after LST, no significant residual tensile stresses were observed, with the stresses

even lower than those of untreated surfaces. Ahmed et al. [28] found that laser surface treatment applied to AISI 304 induces topographic changes and modifies the surface microstructure, while also creating oxide layers between the laser grooves due to the thermal effects. Following LST, no evidence of ferrite precipitates or phase transformation was detected, indicating that LST does not affect the phase transformation of the textured samples. The friction coefficient could be improved in the hard coatings. Li [29] reported that the coefficient of friction of uncoated Al_2O_3-TiC substrate is 0.07 and it decreases to 0.04 under optimal conditions. The uncoated silicon substrate has a coefficient of friction of about 0.4. However, with optimal coating parameters, a significant improvement is observed, reducing the coefficient of friction to 0.2 [30].

In general, the above studies demonstrate the effectiveness of laser surface modification followed by heat treatment in driving the hydrophilic-to-hydrophobic transition in various common engineering metals and alloys. Hydrophobic surfaces offer several key advantages, including enhanced corrosion resistance and reduced friction, which are particularly beneficial for materials such as 316L stainless steel, which is commonly used in demanding environments. Accordingly, this study evaluated the effects of laser surface modification and post-heat treatment on the surface properties, corrosion resistance, and wear performance of 316L stainless steel specimens. The experimental results demonstrated that laser treatment at 500 mm/s, followed by heat treatment at 150 °C for 6 h, produced a hydrophobic surface with a contact angle of 138.0°, superior wear resistance, and enhanced corrosion resistance.

2 Experimental material and procedures

The 316L stainless steel with a composition, in wt.%, of steel-16% Cr-14% Ni-3% Mo-2% Mn was obtained from Yong-Xu Machinery Corporation, Taiwan. 316L stainless steel (PM2-200SA) plates were ground sequentially with 120-grit to 1500-grit sandpaper to remove surface oxides and then polished using a suspension of aluminum oxide powder with a particle size of 1 μm. After polishing, the samples were treated using a UV laser (Coherent AVIA 355–7000, USA) with a wavelength of 355 nm, a beam quality factor (M^2) of 1.3, and a spot diameter of 16 μm. The treatment process was performed using a repetition rate of 25 kHz, laser powers ranging from 0.3 to 1 W, scanning speeds ranging from 100 to 900 mm/s, and a scan pitch of 8 μm. The laser-treated samples were then heated at 150 °C on a hot plate (HP-20D, Shin Kwang Machinery Industry Co., Ltd., Taiwan) for 2 to 12 h or aged under ambient conditions for 0 to 14 days. The surface morphologies of the various samples were observed using an optical microscope (OM; HUVITZ HRM-300). The surface roughness was measured using an Alpha-Step profiler (D-300, KLA, USA). The parameter was set at a speed of 0.1 mm/s and measuring length at 1 mm, and the applied load was 0.15 mg. The wettability was evaluated using deionized water droplets with a volume of 1 μL and a contact angle measuring system (OCA-15EC, Germany). The wear resistance was assessed using an abrasion testing machine (POD FM800 10 NT, FULI-FENG Precision Machinery Co., Ltd., Taiwan) with a stainless steel wear wheel. The tests were conducted under wet conditions (water) with a normal load of 1 kg, a rotational speed of 100 rpm, and 1000 wear cycles. The electrochemical characteristics and corrosion behavior of the samples were evaluated in 0.9% NaCl solution using an electrochemical analyzer (CHI 614E, CH Instruments, USA). The tests were performed at 37 °C with a potential range of − 1 to 1 V and a scan rate of 1 mV/s.

3 Results and discussion

Figure 1 presents the surface morphologies of the specimens treated with different laser powers (0.3, 0.5, and 1 W) and scanning speeds (100, 500, and 900 mm/s). Figure 2 shows the surface roughness values of the nine samples. For laser powers of 0.3 W and 0.5 W, all of the samples had a similar low roughness. However, at the highest laser power of 1 W, the surface roughness increased significantly, particularly at the lowest scan speed of 100 mm/s. Figure 3 shows the contact angle measurements of the nine samples immediately after the laser patterning process. Before the laser treatment, the polished specimens showed an average contact angle of approximately 70°. However, after laser processing, all the samples exhibited hydrophilic properties, with contact angles less than 30°. The contact angle decreased (i.e., the surface became more hydrophilic) as the scanning speed decreased because the greater laser input energy increased the surface roughness, which expanded the effective surface area and strengthened the effects of capillary action. For all values of the scanning speed, the contact angle reduced with an increasing laser power due to a further increase in the laser input energy.

To further investigate the hydrophilic-to-hydrophobic transition, the laser-processed samples were subjected to either ambient air exposure or heat treatment. In the former case, the contact angles of the samples were measured daily over a 14-day holding period in air. As shown in Fig. 4, all the samples underwent a change from a hydrophilic surface to a hydrophobic surface after approximately 6 days. The samples processed with lower laser powers (0.3 and 0.5 W) and a scan speed of 500 mm/s showed a hydrophobic surface with a contact angle of approximately 100–110° after 6 days. For the highest laser power of 1 W, the contact angle

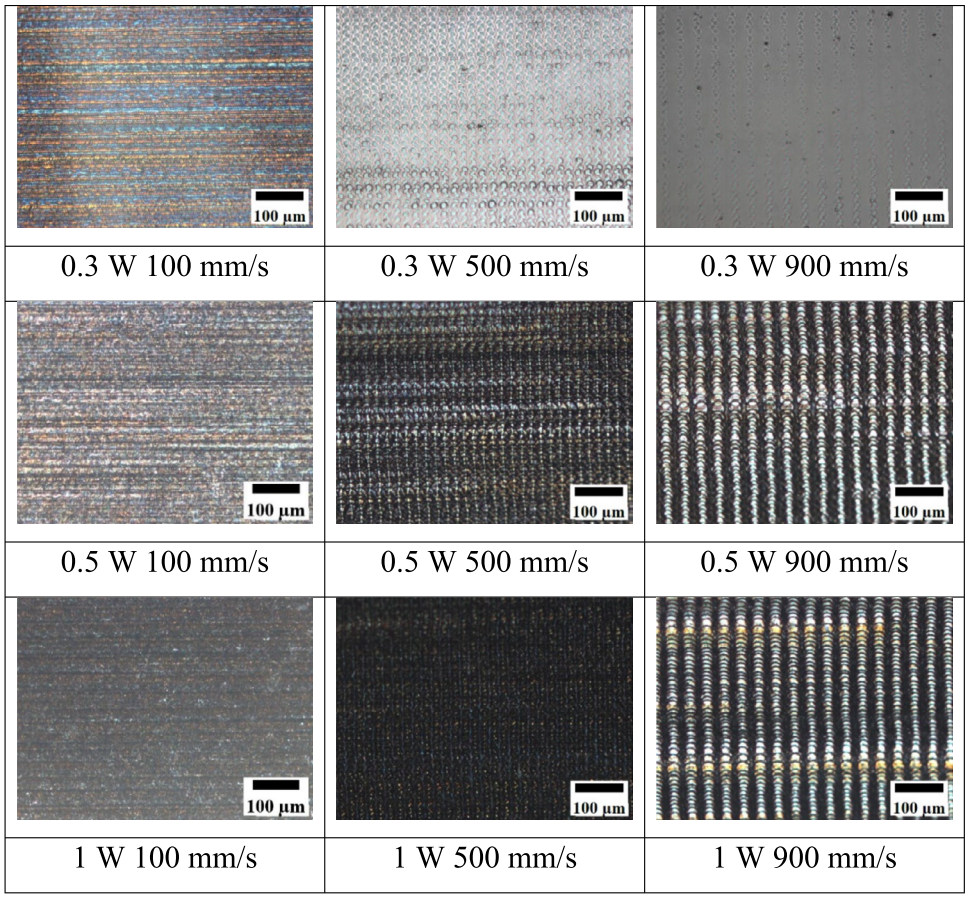

Fig. 1 Optical microscope images showing surface morphologies of 316L specimens following laser modification with different laser powers and scan speeds

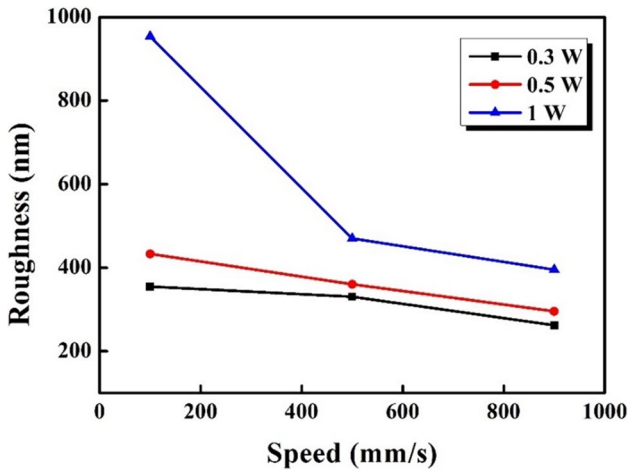

Fig. 2 Surface roughness of 316L specimens following laser modification with different laser powers and scan speeds

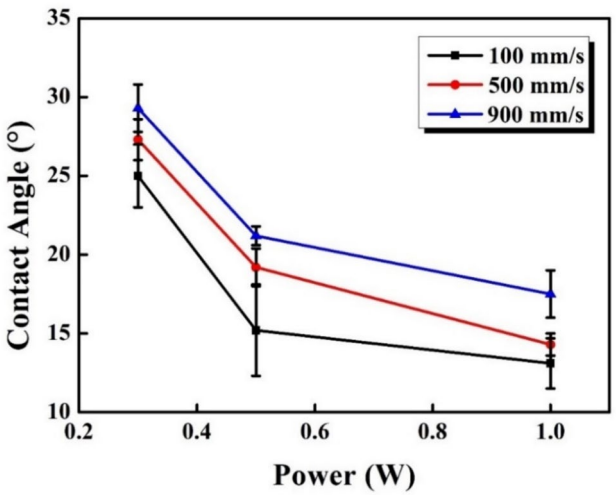

Fig. 3 Variation in contact angle with laser power and scan speed

reached 130.0° after 10 days. In other words, the transition to a steady-state hydrophobic condition took place more slowly than that for the samples processed at a lower laser power, but the final wettability of the surface increased. The initial hydrophilicity of the samples after laser treatment can be attributed to the formation of reactive oxides on the surface. Over time, these oxides react with the water vapor and oxygen content in the ambient air, together with carbon dioxide and organic contaminants, to produce a lower surface energy and hence a greater contact angle [21].

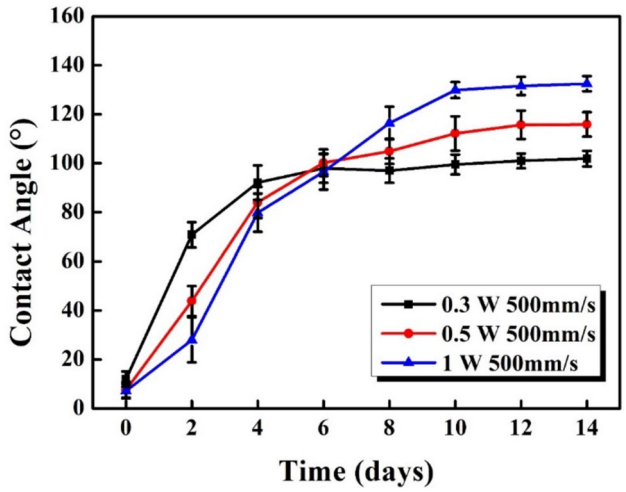

Fig. 4 Variation in contact angle with holding time under ambient conditions for 316L specimens processed using laser powers of **a** 0.3 W, **b** 0.5 W, and **c** 1 W

Figure 5 shows the contact angles of the samples processed using laser powers of 0.3, 0.5, and 1 W and a scanning speed of 500 mm/s, followed by annealing at 100–200 °C for 2 to 12 h. For all values of the laser power, the contact angle increased as the temperature increased from 100 to 150 °C. However, at 200°C, the phase changes and the static contact angle becomes stable early [31]. Thus, 150 °C was determined to be the optimal annealing temperature for all three laser powers. The contact angles of the annealed samples increased slightly in the samples processed using a higher laser power in the initial treatment process. Thus, the maximum contact angle of 138.0° was obtained for the laser sample processed at 1 W. Notably, for this sample, the contact angle reduced slightly as the annealing time increased beyond 6 h as a result of micro-burr structure and surface chemistry. In general, the present findings are consistent with those reported in [7, 9–11, 32], which showed that post-processing techniques such as natural aging, surface chemical modification, and heat treatment can expedite the transition

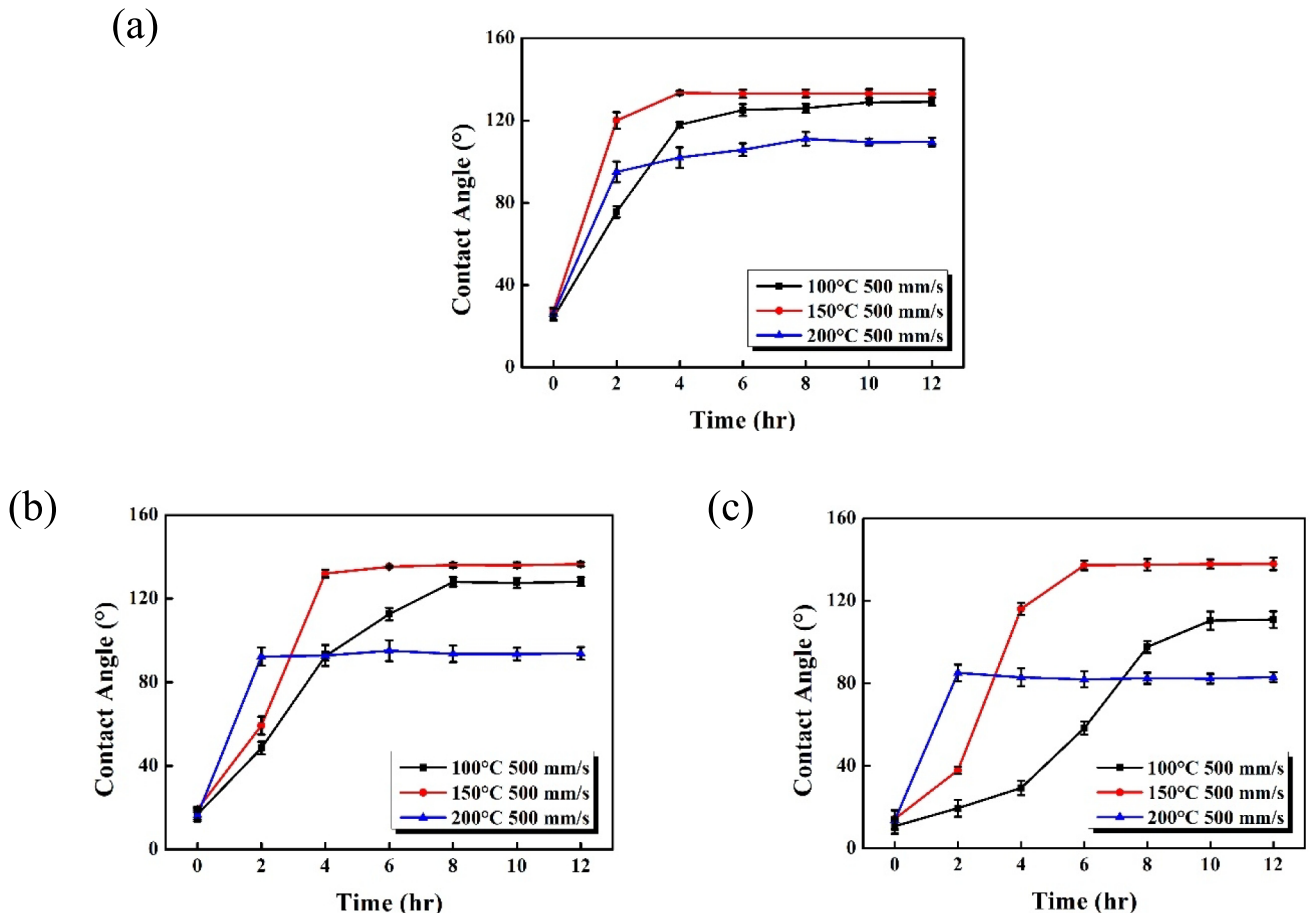

Fig. 5 Variation in contact angle with heating time for annealing temperatures of 100 to 200 °C and laser powers of **a** 0.3 W, **b** 0.5 W, and **c** 1 W

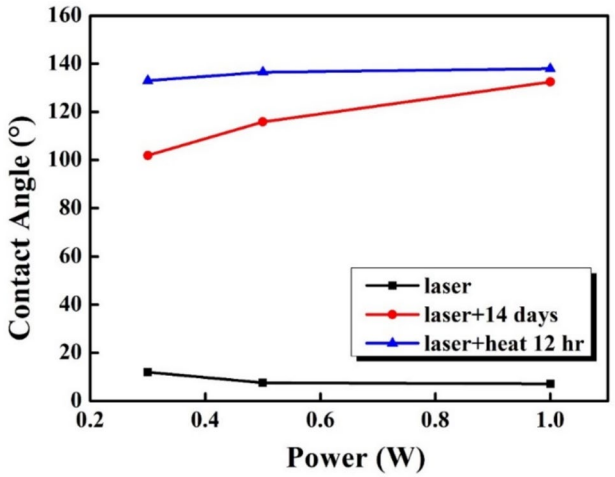

Fig. 6 Variation in contact angle with laser power for samples processed with different treatments

from hydrophilic to hydrophobic surface properties. Figure 6 compares the contact angles of the specimens processed using laser powers of 0.3 W, 0.5 W, and 1.0 W and a scanning speed of 500 mm/s, followed by either aging in air for 14 days or heating at 150 °C for 12 h. The natural aging and heat treatment processes both improved the hydrophobicity of the laser-treated surfaces. However, the annealing process resulted in both a slightly higher contact angle (138.0° vs. 132.5°) and a significantly reduced processing time (12 h vs. 14 days). Therefore, heat treatment offers a more efficient alternative to natural aging for enhancing the wettability of laser-treated 316L stainless steel samples. Accordingly, the wear resistance and electrochemical properties of the samples were investigated for a constant scanning speed of 500 mm/s, an annealing time and temperature of 12 h and 150 °C, and laser powers of 0.3 W, 0.5 W, and 1 W.

Figure 7 shows the variation in the friction coefficients of the various samples over the 1000 cycles of the abrasion wear test. The original polished sample exhibited an average friction coefficient of 0.076. By contrast, the laser-treated samples showed friction coefficients ranging from 0.095 (1 W) to 0.077 (0.3 W). In other words, a higher laser power resulted in a greater friction coefficient, indicating a poorer wear resistance. The 0.3-W sample had a contact angle of 27.3°, while the 1-W sample had a contact angle of 14.3° (Fig. 3). Hence, the wear resistance of the laser-treated samples was positively correlated with the contact angle. Overall, the laser-treated samples exhibited a higher friction coefficient than the polished samples, indicating a reduction in the wear resistance following laser modification. However, the wear resistance was substantially improved in the subsequent heat treatment process. For example, as shown in Fig. 8 for the 1-W sample, the contact angle increased to 138.0°, while the friction coefficient decreased to 0.059. A

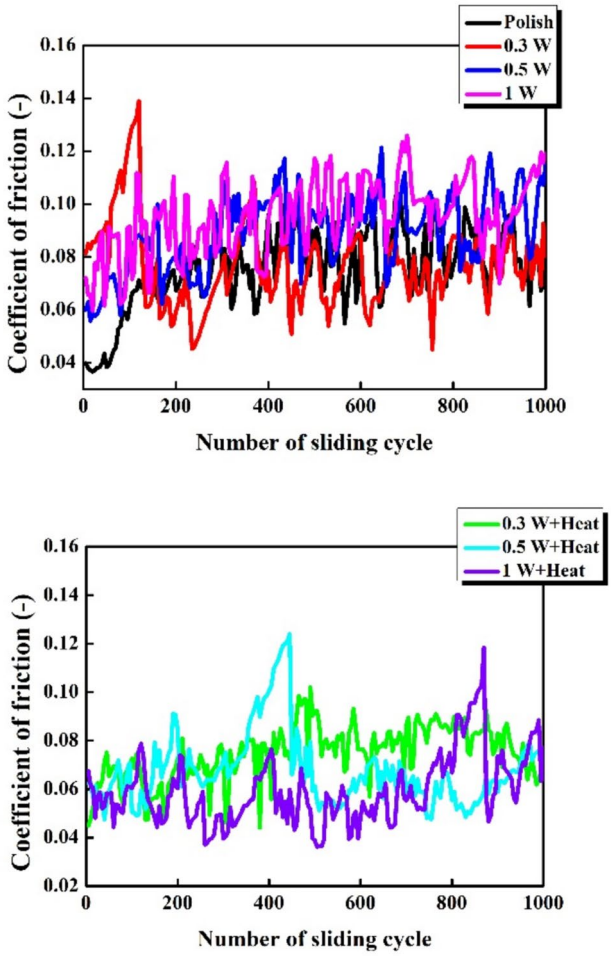

Fig. 7 Friction coefficient profiles for polished, laser-treated, and heat-treated specimens during abrasive wear tests

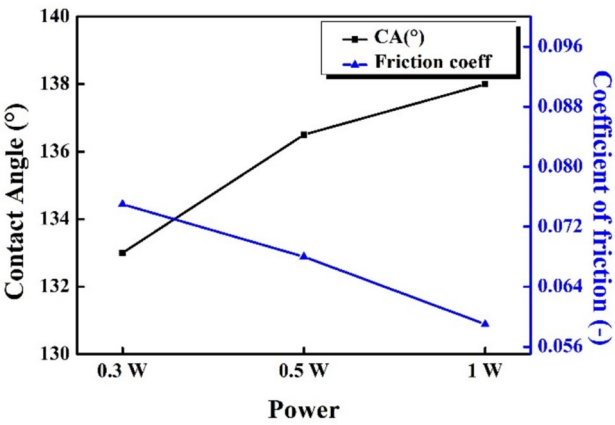

Fig. 8 Relationship between contact angle and coefficient of friction for samples processed using different laser powers

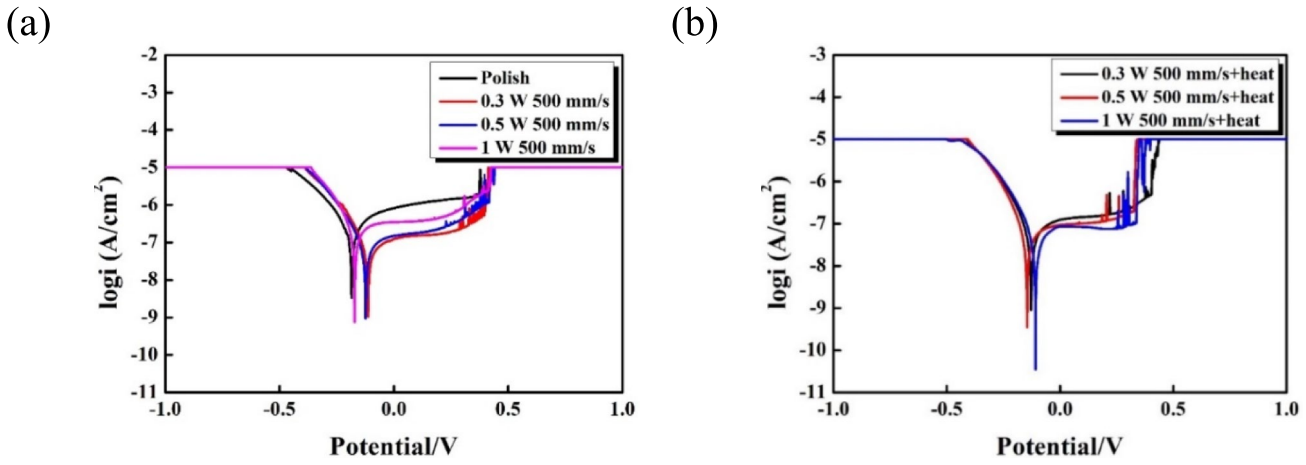

Fig. 9 Tafel plots for **a** polished and laser-treated specimens and **b** laser-treated and heat-treated specimens

similar inverse trend was observed for the 0.3-W and 0.5-W samples. The improvement in the wear resistance can be attributed to the effects of the hydrophobic surface, which creates a thin liquid film at the wear interface. This film provides a lubricating effect that reduces the contact force and friction between the sample surface and the abrasive particles and therefore lowers the coefficient of friction [21, 33–37].

Figure 9a presents the Tafel plots for the polished and laser-treated 316L stainless steel samples. The polished sample exhibited a corrosion current density of 2.98E − 7 A/cm^2. For the laser-treated samples, the corrosion current density increased from 9.60E − 8 to 2.95E − 7 A/cm^2 as the laser power increased from 0.3 to 1 W. In other words, the corrosion resistance decreased as the laser power increased. As stated above, the contact angle reduced from 27.3° to 14.3° as the laser power increased from 0.3 to 1 W. Hence, it is inferred that a higher contact angle results in an enhanced corrosion resistance in the laser-treated samples. All of the laser-treated samples show lower corrosion current densities, and hence improved corrosion resistance, than the original polished sample.

Figure 9b compares the Tafel plots of the laser-treated samples with those of the annealed samples. As the laser power increased from 0.3 to 1 W, the contact angle of the annealed samples rose from 133.0° to 138.0° (Fig. 6) and the corrosion current density decreased from 7.89E − 8 to 5.11E − 8 A/cm^2. Thus, from Eq. (4), the annealed 1-W sample achieved a maximum corrosion inhibition efficiency of 82.8% compared to the original polished sample.

$$\eta IE = \left(I_0 - I_{corr}\right) \div I_0 \times 100\% \quad (4)$$

where I_0 is the corrosion current of the initial sample and I_{corr} is the corrosion current of the treated sample.

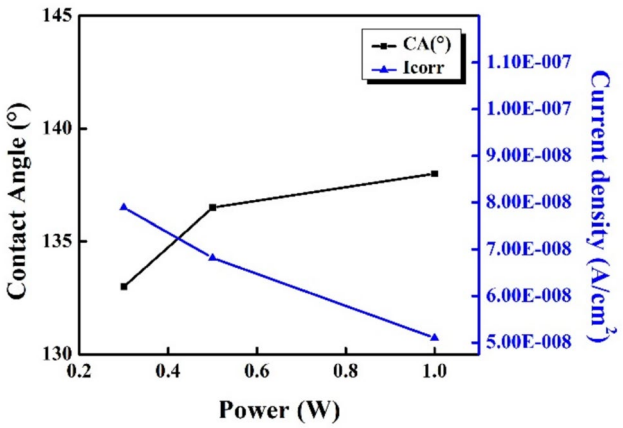

Fig. 10 Relationship between contact angle and corrosion current for samples processed using different laser powers

Overall, the results indicate that combining laser patterning with heat treatment significantly improved the corrosion resistance of the 316L specimens. The enhanced corrosion resistance is most likely due to the more hierarchical surface structure, which includes an air layer that reduces direct contact between the surface and the corrosive agent [38–44].

Figure 10 shows the correlation between the contact angle and the corrosion current density in the sample annealed at 150 °C for 12 h. It can be observed that the contact angle and corrosion current are inversely related. In particular, as the laser power increased from 0.3 to 1 W, the contact angle increased from 133.0° to 138.0° and the corrosion current density decreased from 7.89E − 8 to 5.11E − 8 A/cm^2. Meanwhile, the friction coefficient reduced from 0.075 to 0.059 (Fig. 7). In other words, a positive correlation was observed between the contact angle, wear resistance, and corrosion resistance of the annealed samples. Overall, the

Table 1 Contact angle and corrosion inhibition efficiencies of metal surfaces with various surface treatments

Materials	Laser types	Laser pattern	Post-treatment	Max contact angle	Inhibition efficiency (%)	Ref
Ti-6Al-4V and 316L stainless steel	Ti:sapphire laser system (fs)	Periodic structure	-	124.6° 116.5°	-	[14]
304L stainless steel	Nd:YAG laser (ns)	Grid pattern	-	110°	92.0%	[31]
AISI 4140 mold steel	Ytterbium pulsed laser (ns)	Groove structure	PDMS base curing agent + silicone oil	152.5°	29.5%	[33]
1095 carbon steel	Nanosecond laser marking machine (ns)	Concentric circles pattern	FOTS silane reagent	158.9°	95%	[34]
316L stainless steel	Ytterbium pulsed laser (ns)	Hexagon shape structure	Bioactive glass coatings	-	90.0%	[35]
Aluminum alloy 7075	1030 ultrafast laser source (fs)	Star structure	Natural aging	Above 150.0°	21.4%	[24]
316L stainless steel with Fe-based amorphous alloy coatings	Picosecond laser (ps)	Dimple structure	Poly-perfluoro acrylate	166.5°	74.2%	[25]
316L stainless steel	UV laser (ns)	Groove structure	Natural aging Heat treatment	132.5° 138.0°	82.8%	This work

sample treated with a laser power of 1 W showed the highest contact angle (138.0°), lowest friction coefficient (0.059), and best wear resistance (5.11E − 8 A/cm^2).

Table 1 shows the contact angles and corrosion inhibition efficiencies of metal surfaces processed by various treatments. The results confirm that the proposed UV laser modification process followed by annealing treatment yields a contact angle (138.0°) and inhibition efficiency (82.8%) comparable to (or better than) those of the surfaces processed using alternative approaches.

4 Conclusion

This study has examined the surface roughness, wettability, wear resistance, and anti-corrosion properties of 316L stainless steel specimens processed by laser treatment followed by either aging in air or annealing at temperatures in the range of 100–200 °C. The experimental results support the following conclusions:

1. The increased laser energy produced during laser patterning with either a higher laser power or a slower scanning speed resulted in a greater surface roughness and the formation of a hydrophilic surface with a contact angle of less than 30°.
2. Laser powers of 0.3 W, 0.5 W, and 1 W, combined with a scanning speed of 500 mm/s, followed by heat treatment at 150 °C for 6 h, led to stabilized contact angles of 133.0°, 136.0°, and 138.0°, respectively.
3. After laser patterning and subsequent heat treatment, the friction coefficient of the sample processed with a laser power of 1 W and scanning speed of 500 mm/s decreased from 0.095 to 0.059, indicating a significant improvement in the wear resistance.
4. Laser treatment led to a reduction in the corrosion current. The current was further reduced following subsequent heat treatment. For the sample processed with a laser power of 1 W and scanning speed of 500 mm/s, the current density decreased from 2.95E − 7 A/cm^2 after laser treatment to 5.11E − 8 A/cm^2 after heat treatment, indicating a superior corrosion resistance.

Overall, the results presented in this study demonstrate that laser treatment at a power of 1 W followed by annealing at 150 °C for 6 h enhances the hydrophobicity, wear resistance, and corrosion resistance of 316L.

Author contribution Hsuan-Kai Lin: writing, review, and funding acquisition. Shang-Jen Yang: resources, review, and visualization. Po-Wei Chang: investigation, formal analysis, data collection, visualization. Wei-Hua Lu: original draft, resources, and visualization. Yuan-Jen Chang: review, methodology, and editing.

Funding The authors received financial support provided by the Ministry of Science and Technology of Taiwan, ROC, under Project No. NSTC 112-2637-E-020-004.

Data availability All data generated or analyzed during this study are included in the present article.

Declarations

Ethics approval Not applicable.

Consent to participate Not applicable.

Consent for publication Not applicable.

Competing interests The authors declare no competing interests.

References

1. Lee H-Y, Kim H, Eoh J (2023) Design of type 316L stainless steel 700° C high-temperature piping. Nucl Eng Technol 55(10):3581–3590
2. Baddoo N (2008) Stainless steel in construction: a review of research, applications, challenges and opportunities. J Constr Steel Res 64(11):1199–1206
3. Luo BH, Shum PW, Zhou ZF, Li KY (2010) Preparation of hydrophobic surface on steel by patterning using laser ablation process. Surf Coat Technol 204(8):1180–1185
4. Sciancalepore C, Gemini L, Romoli L, Bondioli F (2018) Study of the wettability behavior of stainless steel surfaces after ultrafast laser texturing. Surf Coat Technol 352:370–377
5. Wu B, Zhou M, Li J, Ye X, Li G, Cai L (2009) Superhydrophobic surfaces fabricated by microstructuring of stainless steel using a femtosecond laser. Appl Surf Sci 256(1):61–66
6. Wang H, Deng D, Zhai Z, Yao Y (2024) Laser-processed functional surface structures for multi-functional applications-a review. J Manuf Process 116:247–283
7. Jagdheesh R, García-Ballesteros J, Ocaña J (2016) One-step fabrication of near superhydrophobic aluminum surface by nanosecond laser ablation. Appl Surf Sci 374:2–11
8. Li X, Jiang Y, Tan X, Zhang Z, Jiang Z, Lian J, Wen C, Ren L (2022) Superhydrophobic brass surfaces with tunable water adhesion fabricated by laser texturing followed by heat treatment and their anti-corrosion ability. Appl Surf Sci 575:151596
9. Martínez-Calderon M, Rodríguez A, Dias-Ponte A, Morant-Miñana MC, Gómez-Aranzadi M, Olaizola SM (2016) Femtosecond laser fabrication of highly hydrophobic stainless steel surface with hierarchical structures fabricated by combining ordered microstructures and LIPSS. Appl Surf Sci 374:81–89
10. Lorenz P, Zajadacz J, Marquardt F, Ehrhardt M, Hommes G, Peter S, Zimmer K (2022) Self-cleaning stainless steel surfaces induced by laser processing and chemical engineering. Procedia CIRP 111:711–714
11. Bizi-Bandoki P, Benayoun S, Valette S, Beaugiraud B (2011) Audouard, Modifications of roughness and wettability properties of metals induced by femtosecond laser treatment. Appl Surf Sci 257(12):5213–5218
12. Young T (1832) An essay on the cohesion of fluids. Philosophical Transactions of the Roya Society of London 1(1):171–172
13. Wenzel RN (1936) Resistance of solid surfaces to wetting by water. Ind Eng Chem 28(8):988–994
14. Cassie A, Baxter S (1944) Wettability of porous surfaces. Trans Faraday Soc 40:546–551
15. Zahid M, Mazzon G, Athanassiou A, Bayer IS (2019) Environmentally benign non-wettable textile treatments: a review of recent state-of-the-art. Adv Coll Interface Sci 270:216–250
16. Kwon MH, Shin HS, Chu CN (2014) Fabrication of a super-hydrophobic surface on metal using laser ablation and electrodeposition. Appl Surf Sci 288:222–228
17. Lin H-K, Li GY, Mortier S, Bazarnik P, Huang Y, Lewandowska M, Langdon TG (2019) Processing of CP-Ti by high-pressure torsion and the effect of surface modification using a post-HPT laser treatment. J Alloy Compd 784:653–659
18. Lin H-K, Cheng Y-H, Li G-Y, Chen Y-C, Bazarnik P, Muzy J, Huang Y, Langdon TG (2022) Study on the surface modification of nanostructured Ti alloys and coarse-grained Ti alloys. Metals 12(6):948
19. Hong TF (2014) Laser surface modification for rapid oxide layer formation on Ti-6Al-4V. J Laser Micro/Nanoeng 9(1):64–67
20. Wan H, Li S, Li J, Liu T, Lin J, Min J (2023) Wettability transition of metallic surfaces from laser-generated superhydrophilicity to water-induced superhydrophobicity via a facile and eco-friendly strategy. Mater Des 226:111691
21. Long J, Zhong M, Zhang H, Fan P (2015) Superhydrophilicity to superhydrophobicity transition of picosecond laser microstructured aluminum in ambient air. J Colloid Interface Sci 441:1–9
22. Zhou Y, Zhang Q, Li X, Wang Y, Guan Y (2024) Mechanical performance of laser-textured metallic surface. J Market Res 33:6084–6089
23. Zhai S, Lu M, Yang Y, Pang M, Ma L (2025) Hydrophobic surface texture air-liquid phase composite assisted laser processing and tribological properties. Appl Surf Sci 681:161534
24. Ngo C-V, Chun D-M (2017) Fast wettability transition from hydrophilic to superhydrophobic laser-textured stainless steel surfaces under low-temperature annealing. Appl Surf Sci 409:232–240
25. Wang Z, Song J, Wang T, Wang H, Wang Q (2021) Laser texturing for superwetting titanium alloy and investigation of its erosion resistance. Coatings 11(12):1547
26. Simson T, Emmel A, Dwars A, Böhm J (2017) Residual stress measurements on AISI 316L samples manufactured by selective laser melting. Addit Manuf 17:183–189
27. Santos AD, Campanelli LC, Silva PS, Vilar R, Almeida MA, Kuznetsov A, Achete CA, Bolfarini C (2019) Influence of a femtosecond laser surface modification on the fatigue behavior of Ti-6Al-4V ELI alloy. Mater Res 22:e20190118
28. Seid Ahmed Y, DePaiva JM, Amorim FL, Torres RD, de Rossi W, Veldhuis SC (2021) Laser surface texturing and characterization of austenitic stainless steel for the improvement of its surface properties. Int J Adv Manuf Technology 115(5):1795–1808
29. Li X, Bhushan B (1988) Micromechanical and tribological characterization of hard amorphous carbon coatings as thin as 5 nm for magnetic recording heads. Wear 220:51–58
30. Li X, Bhushan B (1999) Micro/nanomechanical and tribological characterization of ultrathin amorphous carbon coatings. J Mater Res 14(6):2328–2337
31. Duchemin B, Cazaux G, Gomina M, Bréard J (2021) Temperature-dependence of the static contact angle: a transition state theory approach. J Colloid Interface Sci 592:215–226
32. Ta DV, Dunn A, Wasley TJ, Kay RW, Stringer J, Smith PJ, Connaughton C, Shephard JD (2015) Nanosecond laser textured superhydrophobic metallic surfaces and their chemical sensing applications. Appl Surf Sci 357:248–254
33. Fakhri M, Rezaee B, Pakzad H, Moosavi A (2023) Facile, scalable, and low-cost superhydrophobic coating for frictional drag reduction with anti-corrosion property. Tribol Int 178:108091
34. Ngo CV, Chun DM (2018) Effect of heat treatment temperature on the wettability transition from hydrophilic to superhydrophobic on laser-ablated metallic surfaces. Adv Eng Mater 20(7):1701086
35. Emelyanenko AM, Shagieva FM, Domantovsky AG, Boinovich LB (2015) Nanosecond laser micro-and nanotexturing for the design of a superhydrophobic coating robust against long-term

contact with water, cavitation, and abrasion. Appl Surf Sci 332:513–517
36. Garcia-Giron A, Romano J-M, Batal A, Dashtbozorg B, Dong H, Solanas EM, Angos DU, Walker M, Penchev P, Dimov S (2019) Durability and wear resistance of laser-textured hardened stainless steel surfaces with hydrophobic properties. Langmuir 35(15):5353–5363
37. Wang H, Ma Y, Bai Z, Liu J, Huo L, Wang Q (2022) Evaluation of tribological performance for laser textured surfaces with diverse wettabilities under water/oil lubrication environments. Colloids Surf, A 645:128949
38. Meng S, Yu Y, Zhang X, Zhou L, Liang X, Liu P (2024) Investigations on electrochemical corrosion behavior of 7075 aluminum alloy with femtosecond laser modification. Vacuum 221:112911
39. Wei X, Liao Z, Liang Y, Zhang L, Wang L, Chen B, Shen J (2024) Superhydrophobic Fe-based amorphous alloy coatings with excellent anti-fouling and anti-corrosion properties by picosecond laser texturing. Appl Surf Sci 642:158612
40. Gupta RK, Anandkumar B, Choubey A, George R, Ganesh P, Upadhyaya B, Philip J, Bindra K, Kaul R (2019) Antibacterial and corrosion studies on nanosecond pulse laser textured 304 L stainless steel surfaces. Lasers in Manufacturing and Materials Processing 6:332–343
41. Cholkar A, Chatterjee S, Richards C, McCarthy É, Perumal G, Regan F, Kinahan D, Brabazon D (2024) Biofouling and corrosion protection of aluminum alloys through ultrafast laser surface texturing for marine applications. Adv Mater Interfaces 11(6):2300835
42. Kim B-C, Lim D-W, Kim J-H, Lee H-T (2022) Superhydrophobicity and corrosion resistance of AISI 4140 mold made through nanosecond laser texturing. The International Journal of Advanced Manufacturing Technology 119(7):5119–5130
43. Wang H, Zhuang J, Qi H, Yu J, Guo Z, Ma Y (2020) Laser-chemical treated superhydrophobic surface as a barrier to marine atmospheric corrosion. Surf Coat Technol 401:126255
44. Singh P, Dixit K, Sinha N (2022) A sol-gel based bioactive glass coating on laser textured 316L stainless steel substrate for enhanced biocompatability and anti-corrosion properties. Ceram Int 48(13):18704–18715